

An analytical benchmark for MD codes: testing LAMMPS on the 2nd generation Brenner potential

Antonino Favata¹ Andrea Micheletti² Seunghwa Ryu³ Nicola M. Pugno^{4,5,6}

August 4, 2015

¹ Department of Structural Engineering and Geotechnics
Sapienza University of Rome, Italy
antonino.favata@uniroma1.it

² Dipartimento di Ingegneria Civile e Ingegneria Informatica
University of Rome TorVergata, Italy
micheletti@ing.uniroma2.it

³ Korea Advanced Institute of Science and Technology (KAIST)
ryush@kaist.ac.kr

⁴ Laboratory of Bioinspired and Graphene Nanomechanics
Department of Civil, Environmental and Mechanical Engineering
University of Trento, Italy
nicola.pugno@unitn.it

⁵ Center for Materials and Microsystems
Fondazione Bruno Kessler, Trento, Italy

⁶ School of Engineering and Materials Science
Queen Mary University of London, UK

Abstract

An analytical benchmark is proposed for graphene and carbon nanotubes, that may serve to test whatsoever molecular dynamics code implemented with REBO potentials. By exploiting the benchmark, we checked results produced by LAMMPS (Large-scale Atomic/Molecular Massively Parallel Simulator) when adopting the second generation Brenner potential, we made evident that the code in its current implementation produces results which are offset from those of the benchmark by a significant amount, and provide evidence of the reason.

Keywords: REBO potentials, 2nd generation Brenner potential, LAMMPS, Benchmark

1 Introduction

Molecular dynamics (MD) simulations are nowadays more and more popular in scientific applications, especially in those fields of material science involving nanotechnology and advanced material design. On one side, there are advantages in the speed and accuracy of the simulations, with the model of the potential for atomic interactions being optimized to reproduce either experimental values or quantities estimated by first principles calculations (considered, as a matter of facts, just like experimental results). On the other side, it is more and more frequent to use commercial or open-access codes implementing off-the-shelf potential models, and use them as a black box, without having a precise feeling with the code itself. One of the most used simulator is LAMMPS (Large-scale Atomic/Molecular Massively Parallel Simulator), able to implement several interatomic potentials. By using an analytical discrete mechanical model, we present a benchmark for the equilibrium problem of graphene and carbon nanotubes, which can be applied to any kind of REBO

(reactive empirical bond-order) potential. The analytical condition proposed produces results in complete agreement with First Principles, Density Functional Theory and Monte Carlo simulations. With the aid of this benchmark, we show that LAMMPS code, when implemented with the second generation Brenner potential, produces results which are offset from those of the benchmark by a significant amount, and provide evidence of the reason. The purpose of this letter it is not to just to supply a test for the LAMMPS code, rather, it is to provide a general tool for testing any MD code.

2 An analytical discrete model for equilibrium configurations of FGSs and CNTs

The benchmark solution we propose has been developed within the context of carbon macromolecules, such as Flat Graphene Strips (FGSs) or Carbon Nanotubes (CNTs). When regarded from the point of view of MD, such aggregates are modelled as sets of mass points, whose configuration is described by the Cartesian coordinates of each point with respect to a chosen reference frame; each point is then interacting with the others – at least with the closest ones – and the interaction is captured by a suitable empirical potential, whose shape and parameters are fitted with a set of selected experiments and *ab initio* calculations. The last generation potentials usually take into account multi-particle interactions, up to the third nearest neighbor, which is indispensable to capture the mechanics of complex systems, such as carbon macromolecules.

In order to provide an easy-to-visualize mechanical picture, the perspective we here adopt is not the one of MD, we consider instead the approach of Favata *et al.*[6], where a discrete mechanical model is detailed for 2D carbon allotropes. In this view, the configuration of a molecular aggregate is not identified by the coordinates of the mass points, but rather by a suitable finite list of order parameters. In particular, the conditions of *natural equilibrium* of the aggregate can be determined and expressed in terms of such list and independently of the choice of the REBO potential. As we will see, the prediction of such equations are in total agreement with First Principles, Density Functional Theory and Monte Carlo simulations; moreover, given their generality, they can be exploited to establish benchmark solutions.

In order to understand the physical meaning of the conditions we propose, we summarize some of the results of Favata *et al.*[6]. Starting with the geometry, with reference to Fig. 1, let the axes 1 and 2 be respectively aligned with the armchair and zigzag directions, and let n_1, n_2 be the number of hexagonal cells counted along these axes. Let us consider now the representative cell $A_1B_1A_2B_3A_3B_2A_1$. We note that the sides $\overline{A_1B_1}$ and $\overline{A_3B_3}$ are aligned with the axis 1; the common length of corresponding bonds will be denoted by a , and we will call *a-type* the corresponding bonds. We see that the other four sides have equal length b (*b-type bonds*). We pass to introduce the *bond angles* and, since we intend to consider interactions up to the third neighbor, the *dihedral angles*. As to the bond angles, we notice that they can be of α -*type* and β -*type* (e.g., respectively, $\widehat{A_3B_2A_1}$ and $\widehat{B_2A_1B_1}$; see Fig. 1). As to the dihedral angles, there are five types ($\Theta_1, \dots, \Theta_5$), which can be identified with the help of the colored bond chains in Fig. 1. In conclusion, to determine the deformed configuration of a representative hexagonal cell, no matter if that cell belongs to a FGS or to an achiral CNT, we need to determine the 9-entry *order-parameter substring*:

$$\boldsymbol{\xi}_{sub} := (a, b, \alpha, \beta, \Theta_1, \dots, \Theta_5). \quad (1)$$

The complete order-parameter string for the whole molecular aggregate can be obtained by sequential juxtaposition of substrings.

Due to the geometric compatibility conditions induced by the built-in symmetry (see Favata *et al.*[6] for details), only three of the nine kinematic variables determine the natural configuration, which are chosen to be a, b , and α . In particular, by distinguishing the armchair (superscript A) from the zigzag (superscript Z)

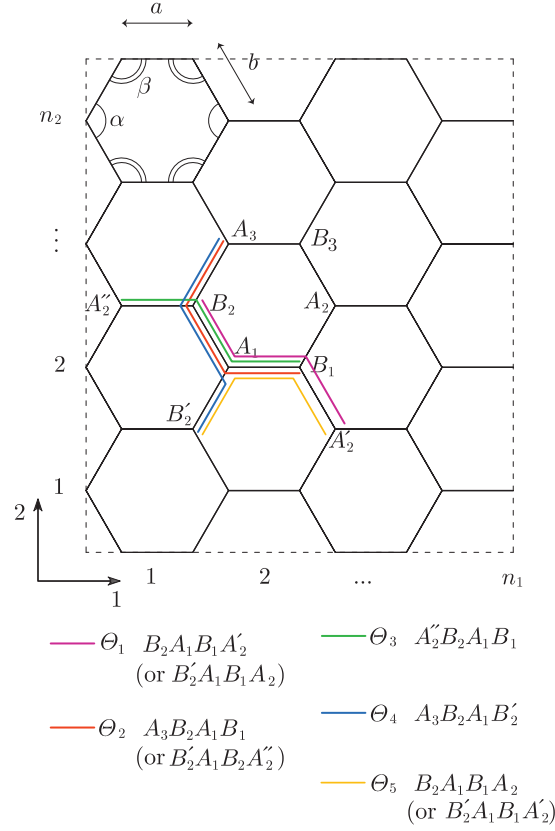


Figure 1: Order parameters in a graphene sheet.

case, the order-parameter substrings are given by, respectively:

$$\begin{aligned}
 \boldsymbol{\xi}_{sub}^A &= (a, b, \alpha, \tilde{\beta}^A(\alpha, \varphi^A), \\
 &\quad \tilde{\Theta}_1^A(\alpha, \varphi^A), \tilde{\Theta}_2^A(\alpha, \varphi^A), 2\tilde{\Theta}_2^A(\alpha, \varphi^A), 0, 0); \\
 \boldsymbol{\xi}_{sub}^Z &= (a, b, \alpha, \tilde{\beta}^Z(\alpha, \varphi^Z), \\
 &\quad \varphi^Z, \tilde{\Theta}_2^Z(\alpha, \varphi^Z), 0, 2\tilde{\Theta}_2^Z(\alpha, \varphi^Z), 0).
 \end{aligned} \tag{2}$$

The explicit form of the functions $\tilde{\beta}^{A,Z}$, $\tilde{\Theta}_1^A$, $\tilde{\Theta}_2^{A,Z}$ is given in Favata *et al.*[6] In (2), $\varphi^A = \pi/n_1$ is the angle between the plane of $A_1B_1B_3$ and the plane of $B_1A_2B_3$ when an armchair CNT is considered, and $\varphi^Z = \frac{\pi}{n_2}$ the angle between the planes of $A_1B_1A_2$ and $A_2B_3A_3$, when a zigzag CNT up is considered. In case of a FGS, we have $\varphi^{A,Z} = 0$, $\tilde{\beta}^{A,Z} = \pi - \alpha/2$, and $\tilde{\Theta}_1^A = \tilde{\Theta}_2^{A,Z} \equiv 0$.

The equilibrium equations turn out to be the following ones:

$$\begin{aligned}
 \sigma_a &= 0, \quad \sigma_b = 0, \\
 \tau_\alpha + 2\beta_{,\alpha} \tau_\beta + \Theta_{1,\alpha} \mathcal{T}_1 + 2\Theta_{2,\alpha} \mathcal{T}_2 + \Theta_{3,\alpha} \mathcal{T}_3 + \Theta_{4,\alpha} \mathcal{T}_4,
 \end{aligned} \tag{3}$$

where $\sigma_a, \sigma_b, \tau_\alpha, \tau_\beta$, and \mathcal{T}_i , are the so-called *nanostresses*, work-conjugate to changes of, respectively, bond lengths, bond angles, and dihedral angles of each type considered. The form of the third of (3) depends on

which of the two achiral CNTs is dealt with; more precisely, we have that

$$\begin{aligned}\tau_\alpha^A + 2\beta^A_{,\alpha} \tau_\beta^A + \Theta_{1,\alpha}^A \mathcal{T}_1^A + 2\Theta_{2,\alpha}^A \mathcal{T}_2^A + \Theta_{3,\alpha}^A \mathcal{T}_3^A &= 0, \\ \tau_\alpha^Z + 2\beta^Z_{,\alpha} \tau_\beta^Z + 2\Theta_{2,\alpha}^Z \mathcal{T}_2^Z + \Theta_{4,\alpha}^Z \mathcal{T}_4^Z &= 0.\end{aligned}$$

Due to their generality, the conditions (3) may serve as a benchmark for any REBO potential. To express the equilibrium equations in terms of the Lagrangian coordinates a, b , and α , it is necessary to introduce the constitutive equations for the stress, which result from the assignment of an intermolecular potential. In the next section, we detail the formulas in the Brenner 2nd generation REBO potential [2] which are needed to solve (3) in terms of the order parameters.

3 REBO potentials

In the Brenner 2nd generation REBO potential, the binding energy V^{REBO} of a molecular aggregate is written as a sum over nearest neighbors:

$$V^{\text{REBO}} = \sum_i \sum_{J < I} V_{IJ};$$

the interatomic potential V_{IJ} is given by the construct

$$V_{IJ} = V_R(r_{IJ}) + b_{IJ}V_A(r_{IJ}), \quad (4)$$

where the individual effects of the *repulsion* and *attraction functions* $V_R(r_{IJ})$ and $V_A(r_{IJ})$, which model pair-wise interactions of atoms I and J depending on their distance r_{IJ} , are modulated by the *bond-order function* b_{IJ} . The repulsion and attraction functions have the following form:

$$\begin{aligned}V_A(r) &= f^C(r) \sum_{n=1}^3 B_n e^{-\delta_n r}, \\ V_R(p) &= f^C(r) \left(1 + \frac{Q}{r}\right) A e^{-\gamma r},\end{aligned}$$

where $f^C(r)$ is a *cutoff function* limiting the range of covalent interactions to nearest neighbors, and where Q, A, B_n, γ , and δ_n , are parameters to be chosen fit to a material-specific dataset. The remaining ingredient in (4) is the *bond-order function*:

$$b_{IJ} = \frac{1}{2}(b_{IJ}^{\sigma-\pi} + b_{JI}^{\sigma-\pi}) + b_{IJ}^\pi,$$

where superscripts σ and π refer to two types of bonds: the strong covalent σ -bonds, between atoms in the same plane, and the π -bonds, which are perpendicular to the plane of σ -bonds. We now describe the functions $b_{IJ}^{\sigma-\pi}$ and b_{IJ}^π .

The role of function $b_{IJ}^{\sigma-\pi}$ is to account for the local coordination of, and the bond angles relative to, atoms I and J , respectively; its form is:

$$\begin{aligned}b_{IJ}^{\sigma-\pi} &= \left(1 + \sum_{K \neq I, J} f_{ik}^C(r_{IK}) G(\cos \theta_{IJK}) e^{\lambda^{IJK}} + \right. \\ &\quad \left. + P_{IJ}(N_I^C, N_I^H) \right)^{-1/2}.\end{aligned}$$

Here, for each fixed pair of indices (I, J) , (a) the cutoff function $f_{IK}^C(r)$ limits the interactions of atom I to those with its nearest neighbors; (b) λ^{IJK} is a string of parameters designed to prevent attraction in some specific situations; (c) function P_{IJ} depends on N_I^C and N_I^H , the numbers of C and H atoms that are nearest neighbors of atom I , and is meant to adjust the bond-order function according to the specific environment

of the C atoms in one or another molecule; (d) according to Brenner et al.[2], for solid-state carbon, the values of both the string λ^{IJK} and the function P_{IJ} are taken null. Finally, function $G(\cos\theta_{IJK})$ modulates the contribution of each nearest neighbor in terms of the cosine of the angle between the IJ and IK bonds; its analytic form is given by three six-order polynomial splines in $\cos\theta$, each of them defined in an interval of the bond angle θ . The corresponding coefficients are determined by fitting each polynomial spline to the values of $G(\cos\theta)$ at certain values of θ .

Function b_{IJ}^π is given a split representation:

$$b_{IJ}^\pi = \Pi_{IJ}^{RC} + b_{IJ}^{DH};$$

the first addendum depends on whether the bond between atoms I and J has a radical character and on whether it is part of a conjugated system, the second depends on dihedral angles. Function b_{IJ}^{DH} is given by

$$b_{IJ}^{DH} = T_{IJ}(N_I^t, N_J^t, N_{IJ}^{\text{conj}}) \times \left(\sum_{K(\neq I, J)} \sum_{L(\neq I, J)} (1 - \cos^2 \Theta_{IJKL}) f_{IK}^C(r_{IK}) f_{JL}^C(r_{JL}) \right),$$

where function T_{IJ} is a tricubic spline depending on $N_I^t = N_I^C + N_I^H$, N_J^t , and N_{IJ}^{conj} , a function of local conjugation, while Θ_{IJKL} is the dihedral angle between the planes of I, J, K and I, J, L .

When the point of view described in Sect. 2 is assumed, the expressions of the potentials have to be specialized and written in terms of the order parameters in the substrings (1). On introducing the potentials V_a and V_b for the a - and b -type bonds, we have, respectively:

$$V_a(a, \beta, \Theta_1) = V_R(a) + b_a(\beta, \Theta_1) V_A(a),$$

$$V_b(b, \alpha, \beta, \Theta_2, \Theta_3, \Theta_4) = V_R(b) + b_b(\alpha, \beta, \Theta_2, \Theta_3, \Theta_4) V_A(b)$$

(see Favata *et al.*[6] for details).

Once this has been done, the nanostresses entering the balance equations (3) can be expressed in terms of the order parameters by means of the following constitutive relations:

$$\begin{aligned} \sigma_a &= V'_R(a) + b_a(\beta, \Theta_1) V'_A(a), \\ \sigma_b &= V'_R(b) + b_b(\alpha, \beta, \Theta_2, \Theta_3, \Theta_4) V'_A(b), \\ \tau_\alpha &= b_{b,\alpha}(\alpha, \beta, \Theta_2, \Theta_3, \Theta_4) V_A(b), \\ \tau_\beta &= \frac{1}{4} (b_{a,\beta}(\beta, \Theta_1) V_A(a) + 2b_{b,\beta}(\alpha, \beta, \Theta_2, \Theta_3, \Theta_4) V_A(b)), \\ \mathcal{T}_1 &= \frac{1}{2} b_{a,\Theta_1}(\beta, \Theta_1) V_A(a), \\ \mathcal{T}_2 &= \frac{1}{2} b_{b,\Theta_2}(\alpha, \beta, \Theta_2, \Theta_3, \Theta_4) V_A(b), \\ \mathcal{T}_3 &= b_{b,\Theta_3}(\alpha, \beta, \Theta_2, \Theta_3, \Theta_4) V_A(b), \\ \mathcal{T}_4 &= b_{b,\Theta_4}(\alpha, \beta, \Theta_2, \Theta_3, \Theta_4) V_A(b). \end{aligned}$$

4 Analytical vs LAMMPS results

The most direct outcomes of our solution are natural geometry and energy, which can be used to check the correctness of whatever MD code. The results obtained by solving equations (3) with Brenner 2nd generation potential are in good agreement with First Principles, Density Functional Theory (DFT) and Diffusion Monte Carlo (DMC) simulations, as Tables 1 and 2 show.

As an application of the possibility of exploiting (3) as a benchmark, we present in Table 3 the radii of a number of CNTs, showing that standard LAMMPS code underestimates them. In Table 4 the values of

the cohesive energy from our solution and those obtained with the use of LAMMPS code when adopting the 2nd-generation Brenner potential are presented; it can be seen that there is a remarkable difference: the cohesive energy is highly overestimated and our benchmark makes evident that the code in its current implementation definitely produces results which are offset from those of the benchmark. The origin of the discrepancies can be found only by a close inspection of LAMMPS source code. In fact, although in Brenner *et al.*[2] it is indicated that the values of the function P_{IJ} should be taken null for solid-state carbon, the code assigns the value 0.027603. This latter value is actually dictated in Table VIII of Stuart *et al.*[10] for AIREBO potentials, due to the additional terms included in this potential. Whenever a LAMMPS user wants to adopt REBO potentials, he needs to change the hard-wired number for the variable PCCf[2][0] in “pair-airebo.cpp”; unfortunately, the LAMMPS manual does not provide any information on this issue, and most studies based on LAMMPS REBO calculations are likely to have underestimation or overestimation of mechanical and geometrical properties presented in our Tables. An example of the use of LAMMPS with 2nd generation Brenner potential is Zhang *et al.*[11]. When the value assigned in Brenner *et al.*[2] is implemented, the LAMMPS code produces the same results as the benchmark solution, letting alone a tiny difference due to numerical effects, as the third column of Tables 3 and 4 undeniably makes evident.

Starting from the geometry and the energy gathered by means of (3), it is possible to obtain secondary quantities. In Table 5 and 6 the Young moduli and the Poisson coefficients are reported: the standard LAMMPS code overestimates the former and underestimates the latter. Our results are in very good agreement with the literature (see e.g. Agrawal *et al.*[1]). The differences between our benchmark and the LAMMPS code with modified parameters are ascribable to numerical effects, more accentuated because Young modulus and Poisson coefficients are quantities not directly evaluated, but rather derived, and an increment of numerical error is foreseeable.

Acknowledgments

AF acknowledges the Italian INdAM-GNFM (Istituto Nazionale di Alta Matematica – Gruppo Nazionale di Fisica Matematica), through “Progetto Giovani 2014 – Mathematical models for complex nano- and bio-materials”. NP is supported by the European Research Council (ERC StG Ideas 2011 BIHSNAM n. 279985 on “Bio-Inspired hierarchical super-nanomaterials”, ERC PoC 2013-1 REPLICA2 n. 619448 on “Large-area replication of biological antiadhesive nanosurfaces”, ERC PoC 2013-2 KNOTOUGH n. 632277 on ‘Super-tough knotted fibres’), by the European Commission under the Graphene Flagship (WP10 “Nanocomposites”, n. 604391) and by the Provincia Autonoma di Trento (“Graphene Nanocomposites”, n. S116/2012-242637 and reg. deliber. n. 2266).

References

- [1] P.M. Agrawal, B.S. Sudalayandi, L.M. Raff, and R. Komanduri. A comparison of different methods of Young’s modulus determination for single-wall carbon nanotubes (SWCNT) using molecular dynamics (MD) simulations. *Comp. Mat. Sci.*, 38(2):271 – 281, 2006.
- [2] D.W. Brenner, O.A. Shenderova, J.A. Harrison, S.J. Stuart, B. Ni, and S.B. Sinnott. A second-generation reactive empirical bond order (REBO) potential energy expression for hydrocarbons. *J. Phys. Cond. Mat.*, 14(4):783, 2002.
- [3] M. F. Budyka, T. S. Zyubina, A. G. Ryabenko, S. H. Lin, and A. M. Mebel. Bond lengths and diameters of armchair single wall carbon nanotubes. *Chem. Phys. Lett.*, 407:266–271, 2005.
- [4] I. Cabria, J. W. Mintmire, and C. T. White. Metallic and semiconducting narrow carbon nanotubes. *Phys. Rev. B*, 67:121406, 2003.
- [5] A. El-Barbary, R. Telling, C. Ewels, M. Heggie, and P. Briddon. Structure and energetics of the vacancy in graphite. *Phys. Rev. B*, 68:144107, Oct 2003.

- [6] A. Favata, A. Micheletti, P. Podio-Guidugli, and N.M. Pugno. Geometry and self-stress of single-wall carbon nanotubes and graphene via a discrete model based on a 2nd-generation REBO potential. <http://arxiv.org/abs/1409.8619>, 2015.
- [7] M. Machón, S. Reich, C. Thomsen, D. Sánchez-Portal, and P. Ordejón. Ab initio calculations of the optical properties of 4- μ m-diameter single-walled nanotubes. *Physical Review B*, 66, 2002.
- [8] V. N. Popov. Curvature effects on the structural, electronic and optical properties of isolated single-walled carbon nanotubes within a symmetry-adapted non-orthogonal tight-binding model. *New J. Phys.*, 6:17, 2004.
- [9] H. Shin, S. Kang, J. Koo, H. Lee, J. Kim, and Y. Kwon. Cohesion energetics of carbon allotropes: Quantum monte carlo study. *The Journal of Chemical Physics*, 140(11):-, 2014.
- [10] S. J. Stuart, A. B. Tutein, and J. A. Harrison. A reactive potential for hydrocarbons with intermolecular interactions. *J. Chem. Phys.*, 112:6472, 2000.
- [11] P. Zhang, L. Ma, F. Fan, Z. Zeng, C. Peng, P.E. Loya, Z. Liu, Y. Gong, J. Zhang, X. Zhang, P.M. Ajayan, T. Zhu, and J. Lou. Fracture toughness of graphene. *Nat. Commun.*, 5, 2014.

Table 1: Cohesive energy (eV/atom)

our benchmark	El-Barbery et al. [5] (First Principles)	Shin et al. 2014 [9] (DMC)
-7.3951	-7.4	-7.464

Table 2: Radii (nm) of small CNTs, comparison with literature

(n, m)	our benchmark	Machón et al. 2002 [7] (DFT)	Cabria et al. 2003 [4] (DFT)	Popov 2004 [8] (TB)	Budyka et al. 2005[3] (DFT)
(3,3)	0.211	0.210	0.212	0.212	-
(4,4)	0.277	-	-	-	0.277
(5,0)	0.208	0.204	0.206	0.205	-

Table 3: Radii

	Our	LAMMPS	LAMMPS
	benchmark	(standard)	(modified)
(n, m)	(nm)	(nm)	(nm)
(3,3)	0.2111	0.2079	0.2110
(4,4)	0.2767	0.2723	0.2766
(5,5)	0.3431	0.3371	0.3404
(6,6)	0.4101	0.4035	0.4100
(7,7)	0.4773	0.4697	0.4773
(8,8)	0.5447	0.5361	0.5447
(10,10)	0.6798	0.6690	0.6798
(12,12)	0.8151	0.8022	0.8151
(18,18)	1.2216	1.2020	1.2215
(25,25)	1.6961	1.6689	1.6960
(5,0)	0.2078	0.2046	0.2076
(6,0)	0.2447	0.2409	0.2446
(7,0)	0.2823	0.2778	0.2821
(8,0)	0.3202	0.3151	0.3201
(9,0)	0.3584	0.3527	0.3583
(10,0)	0.3969	0.3905	0.3967
(12,0)	0.4741	0.4665	0.4739
(15,0)	0.5905	0.5810	0.5904
(20,0)	0.7853	0.7274	0.7852
(30,0)	1.1760	1.1572	1.1759

Table 4: Cohesive energy

(n, m)	Our benchmark (eV/atom)	LAMMPS (standard) (eV/atom)	LAMMPS (modified) (eV/atom)
(3,3)	-7.0137	-7.3838	-7.0137
(4,4)	-7.1695	-7.5569	-7.1695
(5,5)	-7.2463	-7.6422	-7.2462
(6,6)	-7.2898	-7.6905	-7.2896
(7,7)	-7.3167	-7.7204	-7.3166
(8,8)	-7.3346	-7.7403	-7.3345
(10,10)	-7.3560	-7.7640	-7.3558
(12,12)	-7.3678	-7.7771	-7.3676
(18,18)	-7.3829	-7.7038	-7.3827
(25,25)	-7.3887	-7.8003	-7.3886
(5,0)	-6.9758	-7.3417	-6.9759
(6,0)	-7.0969	-7.4763	-7.0969
(7,0)	-7.1715	-7.5593	-7.1715
(8,0)	-7.2212	-7.6144	-7.2212
(9,0)	-7.2560	-7.6531	-7.2560
(10,0)	-7.2814	-7.6812	-7.2813
(12,0)	-7.3151	-7.7186	-7.3149
(15,0)	-7.3432	-7.7499	-7.3431
(20,0)	-7.3656	-7.7747	-7.3655
(30,0)	-7.3819	-7.7927	-7.3818
graphene	-7.3951	-7.8074	-7.3950

Table 5: Young modulus

(n, m)	Our benchmark (GPa)	LAMMPS (standard) (GPa)	LAMMPS (modified) (GPa)
(3,3)	893.9167	987.0102	885.0631
(4,4)	851.4536	944.4810	840.1351
(5,5)	804.6053	901.869	799.7630
(6,6)	800.9298	891.6427	789.8102
(7,7)	793.7379	881.2895	778.2888
(8,8)	784.8784	872.9931	767.9165
(10,10)	768.6379	856.9461	756.7625
(12,12)	756.3044	846.2911	746.5046
(18,18)	735.9332	831.2163	732.5252
(25,25)	726.2650	823.3865	726.4968
(5,0)	948.0854	1046.3569	943.9120
(6,0)	973.0048	1075.4912	968.5679
(7,0)	976.5265	1082.0265	971.5102
(8,0)	969.7954	1076.6910	965.8188
(9,0)	958.1824	1066.6410	954.9396
(10,0)	944.5151	1053.1830	941.3135
(12,0)	916.0510	1025.8253	915.1339
(15,0)	877.5820	986.5745	877.9641
(20,0)	830.0108	940.5973	835.7993
(30,0)	779.7321	890.5147	789.0504

Table 6: Poisson coefficient

(n, m)	Our benchmark	LAMMPS (standard)	LAMMPS (modified)
(3,3)	0.1450	0.1237	0.1563
(4,4)	0.2311	0.2078	0.2388
(5,5)	0.2924	0.25782	0.2963
(6,6)	0.3061	0.27936	0.3115
(7,7)	0.3181	0.2937	0.3318
(8,8)	0.3292	0.3020	0.3458
(10,10)	0.3466	0.3194	0.3526
(12,12)	0.3588	0.3306	0.3626
(18,18)	0.3779	0.3426	0.3740
(25,25)	0.3867	0.3507	0.3790
(5,0)	0.0655	0.0362	0.0661
(6,0)	0.0867	0.0600	0.0840
(7,0)	0.1100	0.0800	0.1105
(8,0)	0.1328	0.1045	0.1306
(9,0)	0.1544	0.1234	0.1511
(10,0)	0.1742	0.1424	0.1737
(12,0)	0.1923	0.1725	0.2032
(15,0)	0.2493	0.2138	0.2446
(20,0)	0.2950	0.2564	0.2835
(30,0)	0.3406	0.2991	0.3261